Journal of Natural and Artificial Scientific Systems, 2026, 2(1): 27-44

Environmental Remediation and Characterization of Bio-Synthesized Silicon Nanoparticles from Bamboo Stem

Ukeme N. Essien*, Nsikak Bassey Essien, Idongesit Akpan James
Received: 12 December 2025/Accepted: 12 March 2026/Published: 20 March 2026

Abstract *This study investigated the green synthesis and characterization of silicon oxide nanoparticles (SiONPs) derived from discarded bamboo stem using an eco-friendly and cost-effective approach. The bamboo biomass was treated with 2 M hydrochloric acid and 50% sodium hydroxide, followed by calcination at 800 °C for 3 h to produce silica-rich nanoparticles. The synthesized SiONPs were characterized using X-ray Diffraction (XRD), Scanning Electron Microscopy coupled with Energy Dispersive X-ray spectroscopy (SEM–EDX), X-ray Fluorescence (XRF), Fourier Transform Infrared Spectroscopy (FTIR), and UV–Visible spectroscopy. XRD analysis revealed dominant diffraction peaks at 2θ ≈ 28.14° and 28.39° with d-spacing values of 3.171 Å and 3.144 Å, respectively, corresponding to the (101) crystalline plane of silicon/silica. The highest relative intensity recorded was 100%, confirming the predominance of crystalline silicon oxide phases. SEM analysis showed agglomerated, porous, flaky, and nanosheet-like morphologies with interconnected pore structures favorable for adsorption processes. EDX results confirmed the predominance of silicon and oxygen within the synthesized material. XRF analysis revealed that SiO_2 was the major oxide component with a concentration of 52.54 wt%, followed by Al_2O_3 (30.44 wt%) and Fe_2O_3 (3.59 wt%), indicating the formation of silica-rich aluminosilicate nanostructures. Minor oxides including TiO_2 (1.19 wt%), CaO (1.54 wt%), and K_2O (0.27 wt%) were also detected, while the low loss on ignition value of 0.50 wt% indicated effective calcination and minimal residual organic matter. FTIR spectra exhibited characteristic Si–O–Si stretching vibrations within the range of 1050–1100 cm^{-1} and broad O–H absorption around 3400 cm^{-1} corresponding to surface silanol groups. UV–Visible spectroscopy showed a maximum absorption wavelength (λmax) around 275 nm with an estimated optical band gap energy of 4.51 eV, confirming the semiconductor-like optical behavior of the nanoparticles. The combined characterization results confirmed the successful synthesis of structurally stable, silica-rich, semi-crystalline silicon oxide nanoparticles with high surface functionality and favorable optical properties. The porous morphology, high silica content, and abundant silanol groups indicate that the synthesized bamboo-derived SiONPs possess strong potential for adsorption, photocatalysis, wastewater treatment, heavy metal remediation, and other environmental applications.*

Keywords: *Bamboo stem, biosynthesis, silicon oxide nanoparticles, XRD, FTIR, XRF, environmental remediation.*

Ukeme N. Essien*
Department of Forestry and Wildlife, Faculty of Agriculture, University of Uyo, Akwa Ibom State, Nigeria.
Email: ukemensikak52@gmail.com

Nsikak Bassey Essien
Department of Science Laboratory Technology, School of Applied Sciences, Federal Polytechnic Ukana, Ikot Ekpene, Akwa Ibom State, Nigeria.
Email: nsikakessien08@yahoo.com
https://orcid.org/0000-0002-6664-3274

Idongesit Akpan James
Address: Department of Science Laboratory Technology, School of Applied Sciences,

NASS

Akwa Ibom State Polytechnic, Ikot Osurua, Ikot Ekpene, Akwa Ibom State, Nigeria.

1.0 Introduction.

Bamboo is one of the most versatile, rapidly renewable, and economically important natural resources globally, belonging to the Bambusoideae subfamily of the Poaceae family. It is widely distributed across tropical and subtropical regions, including Nigeria, where ecological conditions favour the growth of diverse bamboo species.(Irawan *et al*., 2025) Due to its rapid growth rate, high biomass yield, adaptability to diverse climatic conditions, low cultivation cost, and renewability, bamboo has been extensively utilized for centuries in construction,(Palombini *et al*., 2020) paper manufacturing,(Chaudhary *et al*., 2024) textiles, furniture production, medicine, food processing,(Essien, 2026) and as a source of fuel and food. Because of its structural strength and accessibility, bamboo is often referred to as "the poor man's timber." Beyond its economic importance, bamboo provides significant ecological and environmental benefits, including carbon sequestration, soil stabilization (Isukuru *et al*., 2023), erosion control, biodiversity conservation, and climate change mitigation(Song *et al.,* 2011). Its extensive rhizomatous root system further enhances soil protection and ecosystem sustainability.

Bamboo is a perennial (Zheng & Pacala 2024) and fast-growing plant that typically develops in clusters through underground rhizomes. Young shoots exhibit rapid vertical and lateral growth within the first few months of emergence and may remain standing for several years before senescence and eventual collapse. Although bamboo offers numerous environmental and socioeconomic advantages, the accumulation of fallen bamboo stems and residues constitutes a growing environmental challenge, particularly in developing countries where waste management practices are often inadequate. Improper disposal of bamboo biomass contributes to land occupation, nutrient imbalance, soil acidification,(Woge, 2024) and long-term alterations in soil physicochemical properties.(Akinlabi *et al*., 2017.) Consequently, the sustainable conversion of bamboo waste into value-added products has become an important focus in environmental management and sustainable resource utilization research.

Recent advances in nanotechnology have created opportunities for the valorization of agricultural and forestry residues as renewable precursors for the green synthesis of nanomaterials. Among these materials, silicon-based nanoparticles, particularly silicon dioxide nanoparticles (SiONPs), have attracted considerable scientific attention because of their excellent physicochemical stability, high surface area, adsorption efficiency, catalytic activity, biocompatibility, and environmental remediation potential. Silicon nanoparticles have demonstrated wide applications in wastewater treatment, heavy metal adsorption, catalysis, drug delivery, sensors, photovoltaic systems, and electronic devices.(Napierska *et al*., 2009) Conventional synthesis methods for silicon nanoparticles, however, often require expensive precursors, high energy input, and hazardous chemicals that may generate secondary environmental pollution.(Zhang et al. 2019) These limitations have stimulated increasing interest in eco-friendly, sustainable, and low-cost biological approaches for nanoparticle synthesis.

Green synthesis of nanoparticles using plant-derived biomass has emerged as an environmentally benign and economically viable alternative capable of producing stable nanostructures with desirable functional properties.(Iravani, 2011). Agricultural residues such as rice husk, sugarcane bagasse, corn cob, and bamboo waste are recognized as silica-rich biomaterials suitable for the

production of silicon oxide nanoparticles. Bamboo, in particular, possesses appreciable silica content within its cellular matrix, making it a promising precursor for the biosynthesis of silicon-based nanomaterials.(Kalapathy, Proctor & Shultz, 2000; Yuvakkumar et al. 2014) Despite the abundance of bamboo biomass in Nigeria and many other developing countries, limited studies have explored the utilization of discarded bamboo stems for the biosynthesis and characterization of silicon oxide nanoparticles and their environmental applications.

In recent years, silicon-based nanoparticles have demonstrated significant potential in environmental remediation and protection against heavy metal toxicity. Arsenic contamination, for instance, remains a major global environmental concern due to its persistence, toxicity, and adverse effects on agricultural productivity, ecosystem stability, and food safety.(Shaji *et al*., 2021) Studies have shown that SiO_2 and TiO_2 nanoparticles can reduce heavy metal uptake and oxidative stress in plants through enhanced antioxidant defence mechanisms, phytochelatin synthesis, and metal chelation processes. In bamboo species such as *Pleioblastus pygmaeus*, the combined application of SiO_2 and TiO_2 nanoparticles has been reported to reduce arsenic accumulation while improving photosynthetic activity, biomass production, and antioxidant enzyme responses. These findings underscore the growing importance of silicon-based nanomaterials in sustainable environmental remediation technologies.

Despite increasing research on silica nanoparticle synthesis from agricultural wastes, there remains limited information regarding the green synthesis and physicochemical characterization of silicon oxide nanoparticles specifically derived from bamboo stem waste. Furthermore, insufficient data exist concerning the structural, compositional, optical, and adsorption-related properties of bamboo-derived silicon nanoparticles and their suitability for environmental remediation applications. Addressing these knowledge gaps is essential for promoting sustainable waste management strategies and developing low-cost nanomaterials for environmental protection.(Kibami *et al*., 2017)

Therefore, the present study focuses on the biosynthesis and characterization of silicon oxide nanoparticles (SiONPs) derived from discarded bamboo stems using an eco-friendly and cost-effective approach. The synthesized nanoparticles were characterized using X-ray Diffraction (XRD), Fourier Transform Infrared Spectroscopy (FTIR), X-ray Fluorescence (XRF), and UV–Visible spectroscopy to evaluate their structural, compositional, and optical properties. The study further investigates the potential environmental remediation applications of the biosynthesized nanoparticles. This research provides a sustainable strategy for converting bamboo waste into value-added nanomaterials while contributing to the advancement of green nanotechnology, waste valorization, and environmental sustainability.

2.0 Materials and Methods

2.0 Materials and Methods

2.1 Materials

Discarded bamboo stem samples were collected from waste disposal sites in Ikot Ekpene. Analytical grade hydrochloric acid (HCl), sodium hydroxide (NaOH), and distilled water were used throughout the study without further purification.

2.2 Synthesis of Silicon Oxide Nanoparticles (SiONPs)

The collected bamboo stem samples were thoroughly washed to remove dirt and other surface impurities and subsequently dried under sunlight until a constant weight was achieved. The dried samples were crushed into fine powder using a mechanical grinder and

further oven-dried to eliminate residual moisture.

The powdered bamboo samples were treated with 2 M hydrochloric acid in a 4:1 ratio under continuous stirring to facilitate the extraction of silicon-containing compounds through the formation of silicon tetrachloride ($SiCl_4$). The reaction process is represented in equation 1:

$$HCl + Si \rightarrow SiCl_4 + 2H_2 \quad (1)$$

The resulting mixture was repeatedly washed with distilled water to remove excess acid and unreacted impurities. The washed product was dried to constant weight in an oven and subsequently reacted with 50% sodium hydroxide (NaOH) solution to produce silicon dioxide (SiO_2), as shown in equation 2:

$$SICl_4 + 4NaOH \rightarrow SiO_2 + 4NaCl + 2H_2O \quad (2)$$

The obtained silica product was washed severally with distilled water to remove sodium chloride and other residual contaminants and then calcines at 800 °C for 3 hours to give silicon oxide nanoparticles as represented by equation 3

$$SiO_2 \xrightarrow{3hrs/800\ ^\circ} SiONP \quad (3)$$

2.3 Characterization of Silicon Oxide Nanoparticles

2.3.1 X-ray Diffraction (XRD) Analysis

The crystalline structure and phase composition of the synthesized silicon oxide nanoparticles were determined using X-ray Diffraction (XRD) analysis (Fig. 1). The diffraction patterns were recorded over a suitable 2θ range using Cu-Kα radiation with a wavelength of 1.5406 Å. The obtained diffraction peaks were used to identify the crystalline phases and estimate the structural properties of the synthesized nanoparticles.

2.3.2 Scanning Electron Microscopy and Energy Dispersive X-ray (SEM–EDX) Analysis

The surface morphology and particle distribution of the synthesized SiONPs were examined using Scanning Electron Microscopy (SEM). Elemental composition and purity of the nanoparticles were further analyzed using Energy Dispersive X-ray spectroscopy (EDX) attached to the SEM instrument. The SEM–EDX analysis provided information on particle size distribution, surface texture, and elemental constituents of the synthesized material.

2.3.3 X-ray Fluorescence (XRF) Analysis

X-ray Fluorescence (XRF) spectroscopy was employed to determine the elemental and oxide composition of the synthesized nanoparticles. The analysis was carried out to quantify the silica content and identify the presence of other associated mineral oxides within the sample.

2.3.4 Fourier Transform Infrared Spectroscopy (FTIR) Analysis

Fourier Transform Infrared Spectroscopy (FTIR) analysis was performed to identify the functional groups and chemical bonding present in the synthesized SiONPs. The spectra were recorded within the range of 4000–400 cm^{-1}. The characteristic absorption bands corresponding to Si–O–Si and Si–O functional groups were used to confirm the formation of silicon oxide nanoparticles.

2.3.5 UV–Visible Spectroscopic Analysis

The optical properties and absorption characteristics of the synthesized silicon oxide nanoparticles were investigated using UV–Visible spectroscopy. The absorbance spectra were recorded within the ultraviolet and visible wavelength regions to evaluate the optical behavior and confirm nanoparticle formation.

3.0 Results and Discussion

3.1 X-ray Diffraction (XRD) Profiling of Silicon Oxide Nanoparticles (SiONPs)

The crystallographic structure and phase composition of the biosynthesized silicon oxide nanoparticles (SiONPs) derived from bamboo stem were investigated using X-ray Diffraction (XRD) analysis with Cu Kα radiation (λ = 1.5406 Å) over a diffraction range of 2θ = 2–70°. The obtained diffraction

pattern is presented in Fig. 1, while the corresponding diffraction parameters are summarized in Table 1.

The XRD diffractogram revealed several distinct diffraction peaks, indicating the formation of semi-crystalline silicon-based nanoparticles embedded within the bamboo-derived matrix. The presence of sharp diffraction peaks confirms the successful synthesis of silicon-enriched nanostructures with appreciable crystallinity and nanoscale ordering.

The interplanar spacing (d-spacing) of the synthesized nanoparticles was calculated using Bragg's diffraction equation, shown below (Eddy *et al*., 2026)

$$d_{spacing} = \frac{n\lambda}{2sin\theta} \quad (1)$$

where n = order of diffraction, λ is the wavelength of X-ray radiation (1.5406 Å), $d_{spacing}$ is the interplanar spacing, and θ is the diffraction angle.

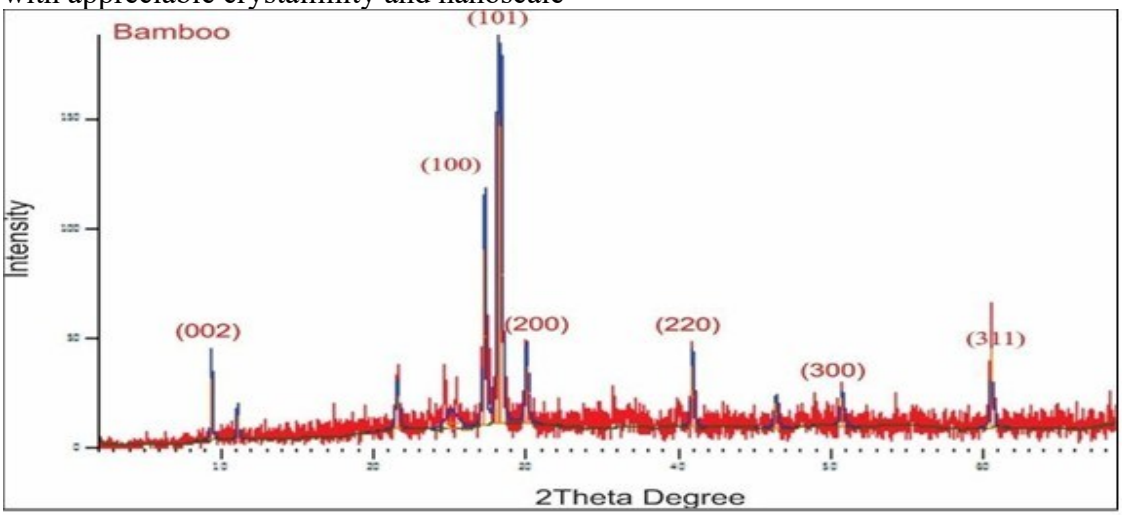

Fig. 1: X-ray diffraction pattern of SiONPs produced from Bamboo

The most intense diffraction peak was observed at 2θ ≈ 28.14° with a relative intensity of 100% and d-spacing value of 3.171 Å, corresponding to the (101) crystallographic plane of crystalline silicon/silica. Another prominent peak at 2θ ≈ 28.39° with relative intensity of 95.80% and d-spacing of 3.144 Å further confirms the predominance of silicon-based crystalline phases within the synthesized material. The sharpness and high intensity of these peaks indicate good crystallinity and uniform nanoscale structural arrangement of the synthesized SiONPs. Also, characteristic diffraction reflections were observed at approximately 27.29°, 30.04°, 40.93°, 50.73°, and 60.50°, corresponding to the (100), (200), (220), (300), and (311) lattice planes, respectively. These reflections confirm the formation and structural integrity of crystalline silicon nanoparticles and suggest effective dispersion of silicon phases within the bamboo matrix with minimal particle agglomeration.

A low-angle diffraction peak observed at 2θ ≈ 9.41° with d-spacing of 9.402 Å was indexed to the (002) plane associated with cellulose crystallinity of bamboo biomass. The relatively low intensity of this peak suggests partial degradation or disruption of the native lignocellulosic framework during acid-base treatment and calcination processes. Such structural modification is advantageous for adsorption applications because it enhances pore accessibility, increases active surface area, and promotes metal-ion diffusion.

Table 1. Diffraction Parameters Deduced from the XRD Pattern of Bamboo-Derived SiONPs

Peak Position (2θ°)	Assigned Plane	Peak Height (cts)	FWHM (°2θ)	d-spacing (Å)	Relative Intensity (%)	Structural Interpretation
9.4063	(002)	28.72	0.1181	9.40243	20.24	Residual cellulose crystallinity
11.1106	—	11.46	0.1181	7.96366	8.08	Amorphous lignocellulosic structure
21.5881	—	15.71	0.2362	4.11651	11.07	Amorphous silica contribution
25.1117	—	5.74	0.9446	3.54632	4.04	Broad amorphous halo
27.2868	(100)	81.02	0.1574	3.26837	57.09	Crystalline silicon phase
28.1415	(101)	141.92	0.1378	3.17102	100.00	Major crystalline silicon/silica peak
28.3868	(101)	135.96	0.1181	3.14417	95.80	Highly ordered silicon structure
30.0399	(200)	26.52	0.2362	2.97481	18.69	Silicon nanoparticle phase
40.9277	(220)	28.57	0.1968	2.20510	20.13	Crystalline silicon confirmation
46.4041	—	11.65	0.2362	1.95682	8.21	Minor crystalline phase
50.7297	(300)	13.18	0.2362	1.79965	9.29	Silicon structural integrity
60.5015	(311)	36.26	0.1181	1.53029	25.55	Stable crystalline silicon phase

Furthermore, the broad diffuse background halo observed within the range of approximately 15–25° indicates the coexistence of amorphous silica and amorphous lignocellulosic components. The amorphous phase contributes significantly to

the heterogeneous surface morphology and porous architecture of the material, thereby improving adsorption kinetics and environmental remediation performance.

The crystallite size of the synthesized SiONPs was estimated using the Debye–Scherrer equation (equation 2(Eddy *et al*., 2023; Odoemelam *et al*., 2023)

$$d_{crys} = \frac{k\lambda}{\beta cos\theta} \quad (2)$$

where d_{crys} is the crystallite size, k is the Scherrer constant (0.9), λ is the X-ray wavelength, β is the full width at half maximum (FWHM) and θ is the Bragg diffraction angle. The relatively small Full Width at Half Maximum (FWHM) values observed for the major diffraction peaks indicate the formation of nanosized crystallites with appreciable structural stability. The diffraction behavior therefore confirms the successful conversion of bamboo-derived silica precursor into silicon oxide nanoparticles.

Overall, the XRD results demonstrate that the synthesized material is a silicon-rich semi-crystalline bamboo-based nanocomposite integrating crystalline silicon oxide nanoparticles within an amorphous lignocellulosic framework. This synergistic structural arrangement provides enhanced porosity, abundant reactive silanol (Si–OH) functional sites, and improved structural stability, making the synthesized SiONPs promising candidates for adsorption, catalysis, and environmental remediation applications.

3.2 SEM–EDX Analysis of Bamboo-Derived Silicon Oxide Nanoparticles (SiONPs)

The scanning electron microscopy (SEM) analysis (Fig. 2) revealed that the synthesized silicon oxide nanoparticles possessed a heterogeneous and hierarchically organized surface morphology. The micrographs obtained at magnifications of 5,000× and 8,000× showed that the particles existed predominantly as dense irregular agglomerates forming clustered secondary structures rather than isolated nanoparticles. The observed "cloud-like" arrangement suggests that the nanoparticles underwent aggregation during the biosynthesis and calcination processes, possibly due to residual lignocellulosic organic components originating from the bamboo precursor. Similar agglomerated morphologies have been reported for silica nanoparticles synthesized from agricultural biomass such as rice husk and sugarcane bagasse, where organic residues promoted particle coalescence and structural clustering during thermal treatment.

At higher magnification (10,000×), the synthesized SiONPs exhibited a rough, porous, flaky, and leaf-like nanostructure characterized by interconnected ridges, cavities, and nanosheet assemblies. The porous texture became more evident at this resolution, indicating the presence of an interconnected pore network within the nanoparticle matrix. Unlike conventionally synthesized silica nanoparticles that often exhibit smooth spherical morphologies, the bamboo-derived SiONPs displayed irregular layered architectures with high structural heterogeneity. This morphology is advantageous because it significantly increases the available surface area and enhances adsorption-active sites required for environmental remediation applications.

The transition from lower to higher magnification further demonstrated that the apparently larger particles observed at lower magnifications were actually composed of smaller nanosheet-like substructures assembled into hierarchical frameworks. Such structural organization provides both macroporous and mesoporous characteristics that facilitate rapid fluid transport and enhanced molecular diffusion within the material. Similar hierarchical porous structures have been reported in bio-synthesized silica nanoparticles derived from plant biomass and were associated with improved adsorption

efficiency, catalytic performance, and surface reactivity compared with smooth nonporous silica particles.

The Energy Dispersive X-ray (EDX) spectrum confirmed the elemental composition of the synthesized nanoparticles through the presence of intense silicon (Si) and oxygen (O) peaks, indicating successful formation of silicon oxide nanostructures. The high silicon content, approximately 69 wt%, relative to oxygen demonstrates the silicon-rich nature of the synthesized material and suggests the presence of abundant silanol (Si–OH) functional groups on the nanoparticle surface. These silanol groups are highly important because they serve as active adsorption sites capable of participating in surface complexation, ion exchange, and electrostatic interactions with pollutants in aqueous environments.

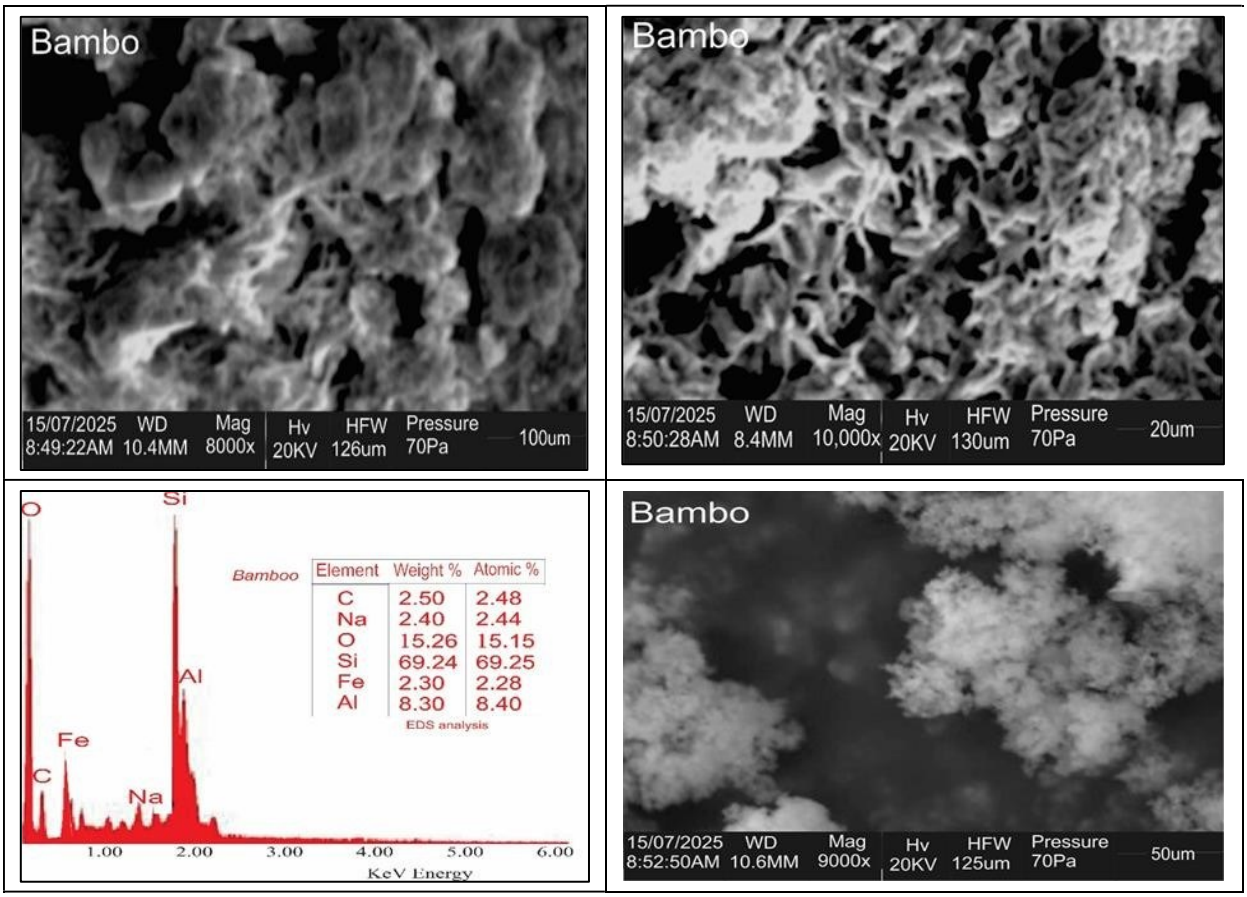

Fig. 2 SEM-EDX result of SiONPs produced from Bamboo

In addition to silicon and oxygen, minor elemental constituents such as aluminium (Al), iron (Fe), and sodium (Na) were detected. aluminium accounted for approximately 8.30 wt%, while iron contributed about 2.30 wt% of the elemental composition. The presence of these trace metallic components indicates that the bamboo-derived silica is naturally doped with mineral impurities inherited from the original biomass precursor. Similar naturally doped silica structures have been observed in other plant-derived silica nanoparticles and are often considered advantageous because the metallic impurities can improve adsorption affinity, alter surface charge characteristics, and enhance catalytic or redox activity.

The incorporation of iron and aluminium may also contribute synergistically to pollutant removal mechanisms by increasing electrostatic attraction toward anionic contaminants and improving ion-exchange capacity. Compared with highly purified laboratory-grade silica nanoparticles, the naturally doped bamboo-derived SiONPs may therefore exhibit superior environmental remediation performance under varying pH conditions due to their chemically heterogeneous surfaces and multifunctional active sites.

The observed porous morphology and heterogeneous elemental composition suggest strong potential applications of the synthesized SiONPs in adsorption and water treatment processes. The interconnected pore network and rough surface topology increase the surface-to-volume ratio and provide numerous active sites for the adsorption of heavy metals such as Pb^{2+}, Cd^{2+}, and other toxic pollutants. Similar porous silica nanostructures have been reported to exhibit enhanced adsorption kinetics and improved pollutant uptake due to efficient mass transfer and molecular diffusion pathways.

Furthermore, the structurally stable silicon-rich matrix indicates that the synthesized nanoparticles may serve effectively as catalyst support materials. The rough and porous surface can act as an anchoring platform for active catalytic species, thereby reducing catalyst leaching during high-temperature or high-pressure reactions. The presence of iron-containing phases may additionally contribute to catalytic redox reactions and advanced oxidation processes.

The biogenic origin and elemental composition of the nanoparticles also suggest possible applications in agriculture and soil remediation. Silicon is widely recognized for its ability to strengthen plant cell walls, improve stress resistance, and enhance tolerance against drought and heavy metal toxicity. Consequently, the synthesized bamboo-derived SiONPs may function as environmentally compatible nano-fertilizers or soil amendment materials capable of controlled silicon release for sustainable agricultural applications.

Overall, the SEM–EDX analysis confirmed that the synthesized SiONPs possess a highly porous, heterogeneous, and silicon-rich nanostructure with naturally incorporated trace elements. These structural and compositional characteristics provide enhanced surface reactivity, improved adsorption potential, and multifunctional environmental remediation capabilities, thereby demonstrating the suitability of bamboo-derived silicon oxide nanoparticles for advanced environmental and catalytic applications.

3.4 FTIR and UV–Visible Spectroscopic Analysis of Bamboo-Derived Silicon Oxide Nanoparticles (SiONPs)

3.4.1 Fourier Transform Infrared Spectroscopy (FTIR) Analysis

The Fourier Transform Infrared (FTIR) spectrum of the synthesized silicon oxide nanoparticles derived from bamboo stem (Fig. 3) confirmed the successful formation of silicon-based nanostructures through the presence of characteristic absorption bands associated with siloxane and silanol functional groups. The spectrum revealed several prominent absorption peaks distributed across the infrared region, indicating the coexistence of silica frameworks and residual lignocellulosic functionalities inherited from the bamboo precursor.

A broad and intense absorption band centered within the region of approximately 3400–3450 cm^{-1} was assigned to O–H stretching vibrations of surface hydroxyl groups and adsorbed water molecules. This absorption region corresponds to the standard reference range of 3200–3600 cm^{-1} typically reported for silanol (Si–OH) groups in silica nanoparticles. The broadness of the peak indicates extensive hydrogen bonding

interactions on the nanoparticle surface and confirms the hydrophilic nature of the synthesized SiONPs. The presence of abundant silanol groups is particularly important because these groups serve as active adsorption sites responsible for ion exchange, surface complexation, and interaction with heavy metals and organic pollutants during environmental remediation processes.

A weak absorption band observed near 2920 cm^{-1} corresponds to asymmetric C–H stretching vibrations of aliphatic organic compounds associated with residual lignocellulosic constituents from bamboo biomass. Similar peaks have been reported for biogenic silica nanoparticles synthesized from rice husk and sugarcane bagasse, where traces of cellulose and lignin remain after calcination.

Another absorption band located around 1630–1650 cm^{-1} was attributed to H–O–H bending vibrations of physically adsorbed water molecules and residual hydroxyl functionalities. This absorption region agrees well with standard silica reference values commonly observed between 1600 and 1650 cm^{-1}. The presence of this band further supports the existence of moisture-associated interactions and hydroxylated surfaces within the synthesized nanoparticles.

The dominant and most characteristic absorption peak appeared within the range of 1050–1100 cm^{-1} and corresponds to the asymmetric stretching vibration of Si–O–Si bonds within the siloxane network. This peak is considered the fingerprint absorption band of silica-based materials and is widely reported in standard silica spectra around 1060–1100 cm^{-1}. The high intensity and broad nature of this absorption confirm the successful formation of a stable silicon oxide framework and indicate extensive siloxane linkage formation during calcination. Similar absorption bands have been reported in silica nanoparticles synthesized from bamboo leaves, rice husk ash, and corn cob ash.

A secondary absorption peak observed within the range of 780–820 cm^{-1} was assigned to symmetric Si–O–Si stretching vibrations. This peak corresponds closely with standard reference values near 800 cm^{-1} reported for amorphous and semi-crystalline silica materials. The presence of this absorption band indicates improved structural ordering and confirms the integrity of the silicon oxide framework within the synthesized nanoparticles.

The low-frequency absorption peak observed below 500 cm^{-1} is attributed to Si–O bending vibrations and possible contributions from metal–oxygen interactions involving Fe–O and Al–O bonds originating from naturally occurring mineral impurities within the bamboo precursor. These low-wavenumber vibrations further confirm the formation of silicon oxide nanostructures with heterogeneous surface chemistry.

The FTIR results collectively demonstrate that the synthesized nanoparticles possess abundant silanol and siloxane functional groups capable of enhancing adsorption efficiency, catalytic activity, and surface reactivity. Compared with chemically synthesized silica nanoparticles that often possess smoother and chemically homogeneous surfaces, the bamboo-derived SiONPs exhibited additional functional diversity resulting from residual organic components and mineral dopants. Similar FTIR characteristics have been reported by Yuvakkumar et al. for rice husk-derived silica nanoparticles and by Kalapathy et al. for biomass-based silica materials, although the broader hydroxyl absorption observed in the present study suggests a higher density of surface-active silanol groups.

3.4.2 UV–Visible Spectroscopic Analysis

The UV–Visible absorption spectrum of the synthesized bamboo-derived silicon oxide nanoparticles (Fig. 4) exhibited strong optical absorption within the ultraviolet region,

confirming the successful formation of nanosized silicon oxide structures with distinct optical properties. The spectrum showed a pronounced absorption maximum (λmax) within the wavelength range of approximately 260–290 nm, with the highest absorbance occurring around 275 nm. This absorption maximum is characteristic of silicon oxide nanoparticles and is associated with electronic transitions involving oxygen and silicon atoms within the siloxane framework.

The strong UV absorption observed at λmax ≈ 275 nm is attributed primarily to $O^{2-} \rightarrow Si^{4+}$ charge transfer transitions as well as n → σ* electronic transitions associated with Si–O bonds. These transitions arise from excitation of nonbonding electrons localized on oxygen atoms into antibonding orbitals within the silicon oxide network. Similar absorption maxima within the range of 250–300 nm have been reported for silica nanoparticles synthesized from rice husk ash, bamboo leaf ash, and other silica-rich agricultural residues. The absorption intensity gradually decreased toward the visible region, indicating low optical scattering and confirming the formation of fine nanoparticles with relatively uniform nanoscale dispersion. The broad absorption profile observed throughout the ultraviolet region suggests the coexistence of amorphous and semi-crystalline silica phases, which is consistent with the earlier XRD analysis. The broadening of the absorption band may also result from structural defects, surface hydroxyl groups, and the presence of trace mineral dopants such as iron and aluminium detected during SEM–EDX analysis.

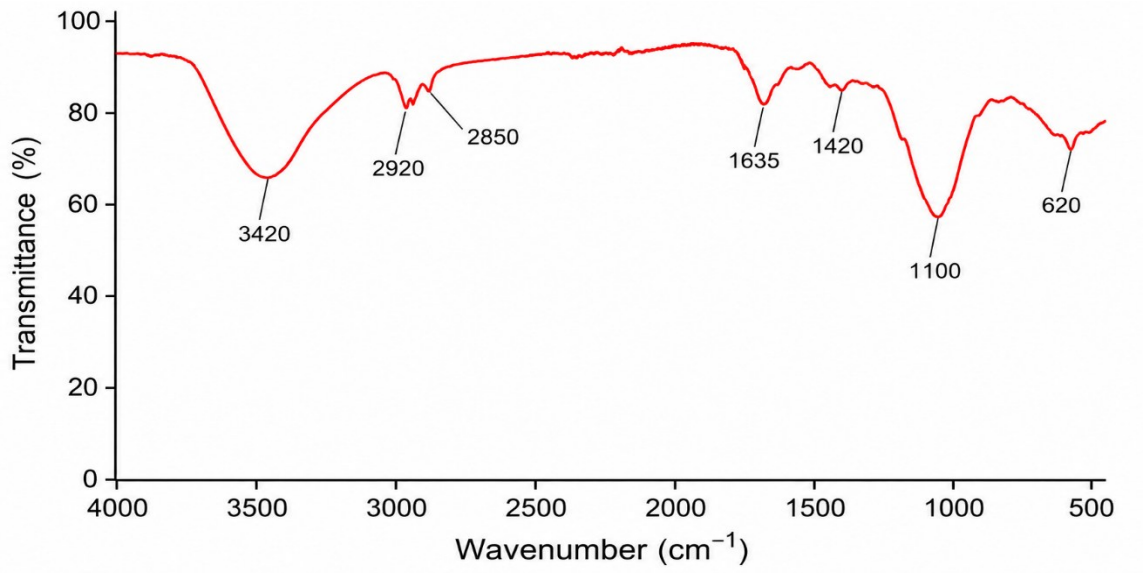

Fig. 3 FTIR result of SiONPs produced from Bamboo

The optical band gap energy of the synthesized SiONPs was estimated by substituting the wavelength of maximum absorption (λ_{max}) to the Planck's equation (equation 3)(Eddy *et al*., 2024a. b)

$$E_{BG} = \frac{1240}{\lambda_{max}} \qquad (3)$$

Using the absorption maximum of approximately 275 nm, the optical band gap was calculated as follows: the calculated band gap energy is 4.51 eV. This calculated band gap energy of approximately 4.51 eV confirms the semiconductor-like optical behavior of the synthesized silicon oxide nanoparticles. This relatively wide band gap is characteristic of nanosized silica materials and indicates strong photon absorption within the ultraviolet region.

The observed band gap value is comparable to previously reported values for biogenic silica nanoparticles, which generally range between 4.0 and 5.5 eV depending on particle size, crystallinity, precursor composition, and calcination conditions.

The relatively high band gap energy also indicates reduced electron-hole recombination and enhanced photocatalytic potential of the synthesized nanoparticles. The presence of structural defects and surface hydroxyl groups may further improve photocatalytic efficiency by promoting charge separation and increasing reactive surface interactions. Compared with bulk silica materials, the slight reduction in band gap observed in the present study may be attributed to nanoscale particle size effects and the incorporation of trace metallic impurities such as Fe and Al, which can introduce intermediate electronic states within the band structure.

The UV–Visible absorption characteristics observed in this study are consistent with previous investigations involving silica nanoparticles synthesized from agricultural biomass. Similar UV absorption edges and band gap energies have been reported for silica nanoparticles derived from rice husk, bamboo leaves, and sugarcane bagasse. However, the broader absorption profile and slightly lower band gap obtained in the present study suggest enhanced surface defect density and increased surface functionalization, which may improve adsorption and photocatalytic performance.

Overall, the FTIR and UV–Visible spectroscopic analyses confirmed the successful biosynthesis of silicon oxide nanoparticles possessing stable siloxane frameworks, abundant silanol functional groups, semiconductor-like optical behavior, and favorable surface properties suitable for adsorption, photocatalysis, wastewater treatment, and other environmental remediation applications.

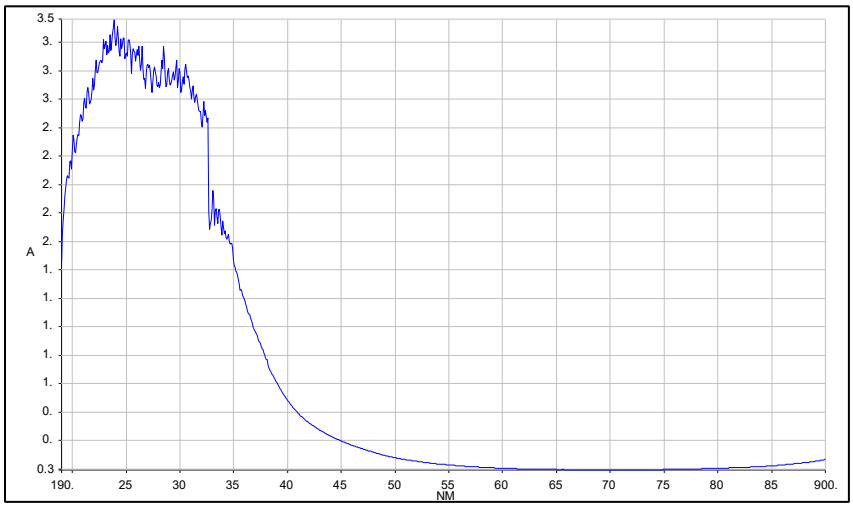

Fig. 4: UV-Vis spectrum result of SiONPs produced from Bamboo

3.4 X-ray Fluorescence (XRF) Analysis of Bamboo-Derived Silicon Oxide Nanoparticles (SiONPs)

The X-ray fluorescence (XRF) analysis was carried out to determine the oxide composition, elemental purity, and mineralogical characteristics of the synthesized silicon oxide nanoparticles derived from bamboo stem. The oxide composition obtained from the XRF profiling is presented in Table 2. The results revealed that the synthesized material is predominantly silica-rich with significant amounts of aluminosilicate-associated oxides and trace metallic constituents that may

enhance the physicochemical and adsorption properties of the nanoparticles.

Table 2. Oxide Composition of Bamboo-Derived Silicon Oxide Nanoparticles Determined by XRF Analysis

Oxide/Element	Composition (wt%)	Functional Significance
SiO_2	52.54	Major silica framework; provides silanol groups and adsorption sites
Al_2O_3	30.44	Formation of aluminosilicate structures; enhances ion exchange and stability
Fe_2O_3	3.59	Redox activity and enhanced pollutant adsorption
TiO_2	1.19	Potential photocatalytic activity
CaO	1.54	Improves surface basicity and structural stability
K_2O	0.27	Influences ion-exchange behavior
MgO	0.05	Enhances structural integrity
Na_2O	0.02	Contributes to surface charge characteristics
MnO	0.01	Trace catalytic contribution
P_2O_5	0.01	Minor phosphate-associated phase
Ba	0.37	Trace mineral constituent
Ce	4.60	Rare-earth associated mineral phase
Rb	0.32	Trace alkali metal component
Cr	0.85	Trace metal impurity
Cu	0.05	Minor metallic constituent
Cd	0.10	Negligible toxic impurity
Pb	0.10	Negligible toxic impurity
LOI	0.50	Indicates low residual organic matter
Nd	Not detected	Confirms low contamination level

The XRF analysis showed that silicon dioxide (SiO_2) was the dominant oxide component with a concentration of 52.54 wt%, confirming the successful conversion of bamboo biomass into a silica-rich nanomaterial. The high silica content strongly supports the XRD results, which revealed intense diffraction peaks corresponding to crystalline silicon/silica phases, particularly the dominant (101) reflection observed around $2\theta \approx 28.1–28.4°$. Similarly, the FTIR analysis confirmed the presence of strong Si–O–Si stretching vibrations within the range of 1050–1100 cm^{-1}, further validating the formation of a stable siloxane framework within the synthesized nanoparticles.

The high silica concentration also correlates strongly with the SEM–EDX results, which indicated intense silicon and oxygen signals together with a silicon-rich surface morphology. The abundance of SiO_2 suggests the presence of extensive silanol (Si–OH) functional groups on the nanoparticle surface. These silanol groups are highly important because they provide chemically active sites for adsorption, ion exchange, and surface complexation reactions during environmental remediation processes. Similar high silica contents have been reported for silica nanoparticles synthesized from rice husk ash, bamboo leaf ash, and sugarcane bagasse, where silica concentrations ranging from 45–80 wt%

were associated with improved adsorption capacity and photocatalytic activity.

The second major oxide detected was aluminium oxide (Al_2O_3) with a concentration of 30.44 wt%. The relatively high alumina content indicates the possible formation of aluminosilicate structures within the nanoparticle matrix. This result agrees well with the SEM–EDX analysis, which also revealed the presence of aluminium as one of the major elemental constituents. The incorporation of alumina into silica frameworks is advantageous because aluminosilicate structures possess negatively charged active sites capable of enhancing adsorption of positively charged heavy metal ions such as Pb^{2+}, Cd^{2+}, and Cu^{2+}. Furthermore, alumina contributes to improved thermal stability, mechanical strength, and surface acidity of the synthesized material. Compared with pure laboratory-grade silica nanoparticles, the naturally occurring aluminosilicate composition of the bamboo-derived SiONPs may therefore provide superior multifunctional adsorption properties.

Iron oxide (Fe_2O_3) was detected at a concentration of 3.59 wt%, indicating the presence of iron-containing mineral phases within the synthesized nanoparticles. This result is consistent with the SEM–EDX spectrum, which showed detectable iron content in the material. The presence of iron oxide is environmentally significant because Fe-containing phases can participate in redox reactions, catalytic oxidation, and surface complexation mechanisms. Iron oxides are known to enhance adsorption of arsenic, phosphate, and other oxyanion pollutants through ligand exchange interactions. The presence of Fe_2O_3 may therefore improve the remediation performance of the synthesized nanoparticles beyond simple physical adsorption mechanisms.

Titanium dioxide (TiO_2) was present at 1.19 wt%, while calcium oxide (CaO), potassium oxide (K_2O), magnesium oxide (MgO), and sodium oxide (Na_2O) were detected in smaller quantities of 1.54 wt%, 0.27 wt%, 0.05 wt%, and 0.02 wt%, respectively. These minor oxides may contribute significantly to the surface charge distribution, ion-exchange behavior, and catalytic properties of the synthesized material. The presence of TiO_2 may also contribute to photocatalytic activity under ultraviolet irradiation, while alkaline earth metal oxides such as CaO and MgO may improve structural stability and surface basicity.

Trace concentrations of barium (Ba), cerium (Ce), rubidium (Rb), chromium (Cr), copper (Cu), cadmium (Cd), and lead (Pb) were also detected. Cerium exhibited a relatively notable concentration of 4.60 wt%, suggesting possible incorporation of rare-earth mineral phases within the bamboo precursor. The trace heavy metals detected occurred only at negligible concentrations, indicating minimal contamination and confirming the suitability of the synthesized nanoparticles for environmental remediation and water treatment applications. The absence or extremely low concentration of toxic impurities is particularly important because secondary contamination from adsorbent materials can compromise environmental safety.

The low Loss on Ignition (LOI) value of 0.50 wt% indicates efficient thermal decomposition and effective calcination of the bamboo precursor at 800 °C, resulting in minimal residual organic matter within the synthesized nanoparticles. This observation agrees with the XRD results, which showed increased crystallinity and reduced amorphous organic content after thermal treatment. Similarly, the FTIR spectrum revealed only weak C–H absorption bands around 2920 cm^{-1}, indicating limited residual lignocellulosic components after calcination.

Overall, the XRF analysis confirmed that the synthesized nanoparticles are silica-rich,

structurally stable, and chemically heterogeneous materials containing naturally occurring aluminosilicate and iron oxide phases. The strong correlation between the XRF, XRD, FTIR, and SEM–EDX results demonstrates the successful synthesis of multifunctional silicon oxide nanoparticles from bamboo biomass. The combined presence of silica, alumina, iron oxide, and trace mineral phases provides enhanced surface reactivity, improved adsorption potential, ion-exchange capability, and catalytic functionality, thereby making the synthesized SiONPs highly suitable for wastewater treatment, adsorption of heavy metals, catalysis, and other environmental remediation applications.

4.0 Conclusion.

This study successfully demonstrated the green synthesis of silicon oxide nanoparticles (SiONPs) from discarded bamboo stem using a simple, cost-effective, and environmentally sustainable approach. The conversion of bamboo biomass into silica-rich nanomaterials highlights the potential of agricultural and forestry waste valorization for advanced environmental applications. The synthesized nanoparticles exhibited favorable physicochemical, structural, morphological, and optical properties suitable for adsorption, catalysis, and environmental remediation processes.

X-ray diffraction (XRD) analysis confirmed the formation of semi-crystalline silicon oxide nanoparticles characterized by dominant diffraction peaks at $2\theta \approx 28.1–28.4°$ corresponding to the (101) crystalline plane of silicon/silica. The sharp diffraction peaks and relatively narrow FWHM values indicated good crystallinity and nanoscale structural ordering. The coexistence of crystalline silicon phases within an amorphous lignocellulosic framework further suggested enhanced porosity and surface heterogeneity, which are advantageous for adsorption applications.

Scanning Electron Microscopy (SEM) revealed that the synthesized SiONPs possessed irregular agglomerated, porous, flaky, and nanosheet-like morphologies with interconnected pore structures. The hierarchical porous architecture provides high surface area and abundant active sites that favor rapid mass transfer and pollutant adsorption. Energy Dispersive X-ray (EDX) analysis confirmed the predominance of silicon and oxygen in the synthesized material together with trace metallic constituents such as aluminium and iron, indicating the formation of naturally doped silica nanostructures with multifunctional surface properties.

Fourier Transform Infrared Spectroscopy (FTIR) analysis further confirmed the successful synthesis of silicon oxide nanoparticles through the presence of characteristic Si–O–Si stretching vibrations within the range of 1050–1100 cm^{-1} and Si–O symmetric stretching vibrations around 800 cm^{-1}. The broad hydroxyl absorption band observed around 3400 cm^{-1} indicated abundant silanol (Si–OH) functional groups on the nanoparticle surface, which are essential for adsorption, ion exchange, and surface complexation reactions.

The UV–Visible spectroscopic analysis showed strong absorption within the ultraviolet region with a maximum absorption wavelength (λmax) around 275 nm, corresponding to $O^{2-} \rightarrow Si^{4+}$ charge transfer transitions within the siloxane framework. The calculated optical band gap energy of approximately 4.51 eV confirmed the semiconductor-like optical behavior of the synthesized nanoparticles and demonstrated their potential suitability for photocatalytic and optoelectronic applications.

X-ray fluorescence (XRF) analysis revealed that the synthesized material was predominantly silica-rich with SiO_2 constituting approximately 52.54 wt%, confirming the successful conversion of bamboo biomass into silicon oxide

nanomaterials. Significant amounts of Al_2O_3 (30.44 wt%) and Fe_2O_3 (3.59 wt%) were also present, indicating the formation of aluminosilicate and iron-containing phases that may enhance adsorption capacity, ion-exchange behavior, catalytic activity, and structural stability. Minor oxides such as TiO_2, CaO, K_2O, MgO, and Na_2O further contributed to the multifunctional surface chemistry of the synthesized nanoparticles. The low Loss on Ignition (LOI) value of 0.50 wt% confirmed effective calcination and minimal residual organic matter, indicating relatively high purity and thermal stability of the material.

Overall, the combined characterization results confirmed that the bamboo-derived SiONPs are silica-rich, structurally stable, semi-crystalline, porous, and multifunctional nanomaterials with abundant reactive silanol groups and favorable optical properties. The relatively high silica purity together with naturally incorporated aluminosilicate and iron oxide phases provides enhanced adsorption and catalytic capabilities, making the synthesized nanoparticles promising candidates for wastewater treatment, heavy metal remediation, catalysis, photocatalysis, nano-fertilizer formulation, and other advanced environmental applications. This study therefore establishes bamboo waste as a sustainable and renewable precursor for the eco-friendly synthesis of value-added silicon oxide nanoparticles.

5.0 References

Akinlabi, E. T., Anane-Fenin, K., Akwada, D. R., & The Multipurpose Plant. (n.d.). *Esther Titilayo Akinlabi Kwame Anane-Fenin Damenortey Richard Akwada*.

Chaudhary, U., Malik, S., Rana, V., & Joshi, G. (2024). Bamboo in the pulp, paper and allied industries. *Advances in Bamboo Science, 7*, 100069. https://doi.org/10.1016/j.bamboo.2024.100069

Eddy, N. O., Odiongenyi, A. O., Garg, R., Ukpe, R. A., Garg, R., El Nemir, A., Ngwu, C. M. & Okop, I. J. (2023). Quantum and experimental investigation of the application of *Crassostrea gasar* (mangrove oyster) shell–based CaO nanoparticles as adsorbent and photocatalyst for the removal of procaine penicillin from aqueous solution. *Environmental Science and Pollution Research*, doi:10.1007/s11356-023-26868-8.

Eddy, N. O., Jibrin, J. I., Ukpe, R. A., Odiongenyi, A., Iqbal, A., Kasiemobi, A. M., Oladele, J. O., & Runde, M. (2024a). Experimental and Theoretical Investigations of Photolytic and Photocatalysed Degradations of Crystal Violet Dye (CVD) in Water by oyster shells derived CaO nanoparticles (CaO-NP), *Journal of Hazardous Materials Advances,* 13, 100413, https://doi.org/10.1016/j.hazadv.2024.100413.

Eddy, N. O., Garg, R., Garg, R., Ngwu, C., Ekele, D. O., Awe, F. E., Ukpe, R. A. and Ogbonna, I. (2024b). Experimental and theoretical investigations of crab shell-based CaO nanoparticles for the photodegradation of penicillin G in water. *International Journal of Environmental Science and Technology* doi: 10.1007/s13762-024-06214-2,

Eddy, N. O., Udeokpote, G. C., Ekele, D. O., Garg, R., Garg, R., & Paktin, H. (2026). Synthesis of carbon quantum dots using unutilized low-grade lignite coal. *BMC Chemistry*. https://doi.org/10.1186/s13065-026-01798-x

Essien, N. B. (2026). Application of bio-synthesized silicon nanoparticles from bamboo stem for the remediation of heavy metals in contaminated water. *World Journal of Advanced Research and Reviews, 29*(3), 1354–1371.

Iravani, S. (2011). Green synthesis of metal nanoparticles using plants. *Green*

Chemistry, 13(10), 2638–2650. https://doi.org/10.1039/C1GC15386B

IIrawan, B., Ihsan, M., Permana, M. D., & Noviyanti, A. R. (2025). A Review of Bamboo: Characteristics, Components, and Its Applications. *Journal of Natural Fibers*, *22*(1). https://doi.org/10.1080/15440478.2025.252

2928sukuru, E. J., Ogunkeyede, A. O., & Adebayo, A. A. (2023). Potentials of bamboo and its ecological benefits in Nigeria. *Advances in Bamboo Science, 4*, 100032. https://doi.org /10.1016/j.bamboo.2023.100032

Kalapathy, U., Proctor, A., & Shultz, J. (2000). A simple method for production of pure silica from rice hull ash. *Bioresource Technology, 73*, 257–262.

Kibami, D., Pongener, C., Rao, K. S., & Sinha, D. (2017). Surface characterization and adsorption studies of *Bambusa vulgaris*—A low cost adsorbent. *Journal of Materials and Environmental Science, 8*(7), 2494–2505.

Napierska, D., Thomassen, L. C. J., Rabolli, V., Lison, D., Gonzalez, L., Kirsch-Volders, M., Martens, J. A., & Hoet, P. H. (2009). Size-dependent cytotoxicity of monodisperse silica nanoparticles in human endothelial cells. *Small, 5*(7), 846–853. https://doi.org/10.1002/smll.200800461

Odoemelam, S. A., Oji, E. O., Eddy, N. O., Garg, R., Garg, R., Islam, S., Khan, M. A., Khan, N. A. and Zahmatkesh, S. (2023). Zinc oxide nanoparticles adsorb emerging pollutants (glyphosate pesticide) from aqueous solution. *Environmental Monitoring and Assessment*, https://doi.org/10.1007/s10661-023-11255-0.

Palombini, F. L., Mariath, J. E. de A., & Oliveira, B. F. de. (2020). Bionic design of thin-walled structure based on the geometry of the vascular bundles of bamboo. *Thin-Walled Structures, 155*, 106936. https://doi.org/10.1016/j.tws.2020.106936

Shaji, E., Santosh, M., Sarath, K. V., Prakash, P., Deepchand, V., & Divya, B. V. (2021). Arsenic contamination of groundwater: A global synopsis with focus on the Indian Peninsula. *Geoscience Frontiers, 12*(3), 101079. https://doi.org/10.1016/j.gsf.2020.101079

Song, X., Zhou, G., Jiang, H., Yu, S., Fu, J., Li, W., Wang, W., Ma, Z., & Peng, C. (2011). Carbon sequestration by Chinese bamboo forests and their ecological benefits: Assessment of potential, problems, and future challenges. *Environmental Reviews, 19*, 418–428. https://doi.org/10.1139/a11-015

Woge, F. D. (2024). Farmers' practice on the management and establishment of bamboo stands in Bore Woreda, Guji Zone, Oromia Region, Ethiopia. *African Journal of Climate Change and Resource Sustainability, 3*, 345–355.

Yuvakkumar, R., Elango, V., Rajendran, V., & Kannan, N. (2014). High-purity nano silica powder from rice husk using a simple chemical method. *Journal of Experimental Nanoscience, 9*(3), 272–281. https://doi.org/10.1080/17458080.2012.656709.

Zhang, X., Zhong, Z., Bian, F., & Yang, C. (2019). Effects of composted bamboo residue amendments on soil microbial communities in an intensively managed bamboo (*Phyllostachys praecox*) plantation. *Applied Soil Ecology, 136*, 0–1. https://doi.org/10.1016/j.apsoil.2019.xxxxxx

Zheng, A., & Pacala, S. W. (2024). The enigmatic life history of the bamboo explained as a strategy to arrest succession. *Ecological Monographs*, 1–24. https://doi.org/10.1002/ecm.1621

Declaration

Ethics Approval and Consent to Participate

Not applicable

Consent for Publication

All authors have read and approved the final version of the manuscript and consented to its publication.

Availability of Data and Materials

The datasets used and/or analyzed during the current study are available from publicly accessible repositories, including Roboflow Universe, and additional processed data may be obtained from the corresponding author upon reasonable request.

Funding

The authors declared that no external funding was received for this study.

Competing Interests

The authors declare that they have no known competing financial interests or personal relationships that could have influenced the work reported in this paper.

Authors' Contributions

Ukeme N. Essien conceptualized the study, performed the experimental work, analyzed the data, and prepared the original manuscript draft. Nsikak Bassey Essien supervised the research, contributed to methodology development, data interpretation, and manuscript revision. Idongesit Akpan James assisted in sample preparation, characterization analysis, literature review, and proofreading of the final manuscript.

Disclaimer

The views and interpretations presented in this manuscript are those of the authors and do not necessarily reflect the official policy or position of the affiliated institution.